Temperature-Driven Enhancement of the Stimulated Emission Rate in Terahertz Quantum Cascade Lasers

Asaf Albo and Yuri V. Flores

***Abstract*— We analyze the temperature dependence of the light output power of terahertz quantum cascade lasers (THz-QCLs) and demonstrate an enhancement of the stimulated emission rate triggered by thermally activated electron leakage from the lower laser level into the continuum. Contrary to common sense expectation, we find that this leakage channel contributes positively to the temperature performance of THz-QCLs. We show that this leakage mechanism is the missing component to explain the full temperature dependence of the light output power as it counteracts the population inversion reduction that arises from non-radiative electron scattering from the upper into the lower laser state. We analyze experimental light output power versus temperature data for a 3.87-THz-emitting device with highly diagonal optical transition over a wide temperature range (10–180 K) and show how thermally activated leakage of electrons from the lower laser level leads to a nearly constant output power up to a temperature of ∼120 K. These results open the question if new design approaches that exploit this effect can be developed in order to demonstrate devices with higher maximum operating temperature.**

***Index Terms*— Quantum cascade laser (QCL), semiconductor device modeling, submillimeter wave laser.**

I. Introduction

TERAHERTZ quantum cascade lasers (THz-QCLs) are unique light sources in the submillimeter wavelength range with enormous potential for novel, groundbreaking scientific instrumentation as well as novel commercial applications. Light generation in THz-QCLs is achieved by radiative transitions between quantum-well states within the conduction band of a semiconductor heterostructure. Under a certain bias the ideal operation of a THz-QCL assumes that an electron injected externally into the device will generate multiple photons –one in each "energy cascade"– while transporting through the heterostructure. However, alternative scattering paths that deviate electron transport from the ideal picture are also present and have a considerable effect on the temperature performance of devices. The maximum operating temperature of THz-QCLs is currently limited to values up to T_{max}∼200 K in pulsed operation mode [1] and its improvement has decelerated in recent years. Besides technological factors, the slow progress in T_{max} is also related to an incomplete understanding of the temperature-driven electron transport in THz-QCLs. In this context, thermally activated leakage of electrons out of QCL active region states deserves particular attention. Several works of both theoretical and experimental nature have been reported on the topic of electron leakage in mid-IR QCLs, and its huge impact on the performance of devices has been demonstrated [2]–[5]. The review paper of Botez *et al.* [2] is recommended for further references. However, unlike in the mid-IR QCL scientific community, temperature-driven electron leakage has been addressed only marginally in THz-QCL studies. A better understanding of the temperature degradation mechanisms in THz-QCLs would be certainly helpful to optimize design concepts and ultimately contribute to achieve higher values of T_{max}.

In previous contributions we proposed a method to investigate the temperature degradation of THz-QCLs by analyzing the light output power vs. temperature experimental data in terms of activation energies [6]–[8]. The measured activation energies helped to identify the dominant physical mechanisms associated with the performance degradation as the temperature increases. Using this method, we demonstrated that the performance of devices using a vertical radiative transition is strongly limited by electron scattering from the upper- into the lower laser state via thermally activated electron-longitudinal optical (LO) phonon interaction [6]. In addition, we demonstrated that the performance of devices using diagonal radiative transitions degrades due to thermally activated leakage of carriers into the continuum [7] and thermally activated shunt-type carrier leakage through excited confined states [8].

However, those works ([6]–[8]) provide only partial understanding of the temperature-dependent transport mechanisms that define the output power in THz-QCLs. One contradiction between theory and experiment arises when analyzing device LBD of [7], a THz-QCL with highly diagonal radiative transition. A nearly constant light output power up to a temperature of ∼120 K was observed in that work, although a continuously decaying output power is expected as the temperature increases.

To illustrate this discrepancy, we reproduce in Fig. 1 the measured light output power of device LBD together with a theoretical calculation that takes into account carrier

Manuscript received September 18, 2016; revised November 11, 2016; accepted November 15, 2016. Date of publication November 22, 2016; date of current version December 12, 2016. The work of A. Albo was supported in part by MIT-Technion and the Andrew and Erna Finci Viterbi Fellowships. The work of Y. V. Flores was supported by the Research Fellowship Program of the German Research Foundation, DFG under Grant FL945/1-1.

The authors are with the Research Laboratory of Electronics, Massachusetts Institute of Technology, Cambridge, MA 02139 USA (e-mail: asafalbo@gmail.com; yvf@mit.edu).

Color versions of one or more of the figures in this paper are available online at http://ieeexplore.ieee.org.

Digital Object Identifier 10.1109/JQE.2016.2631899

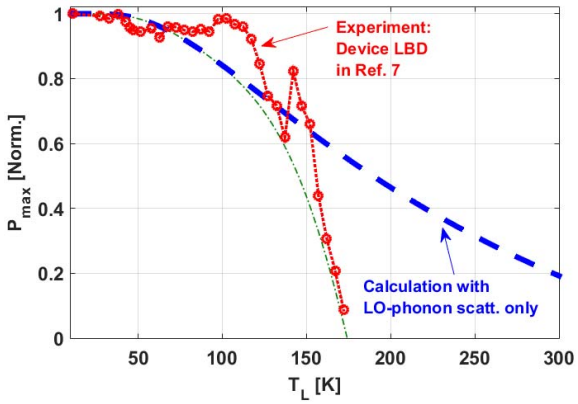

Fig. 1. Measured light output power vs. temperature for device LBD of [7] (red circles) together with a theoretical calculation (dashed blue line) that takes into account thermally activated electron scattering from the upper laser level (ULL) into the lower laser level (LLL) by LO-phonons. The dashed-dotted green line is a guide to the eye for the expected output power behavior when electron scattering from the ULL into the continuum is added to electron- LO-phonon scattering from the ULL into the LLL. This line approximates at low temperatures the expected behavior for ULL to LLL relaxation (dashed blue line), whereas at high temperatures it approximates the expected behavior for thermally activated leakage from the ULL into the continuum [7]. As a result, the dashed-doted green line decays continuously as the temperatures increases and it leads to output power values equal or lower than the dashed blue line.

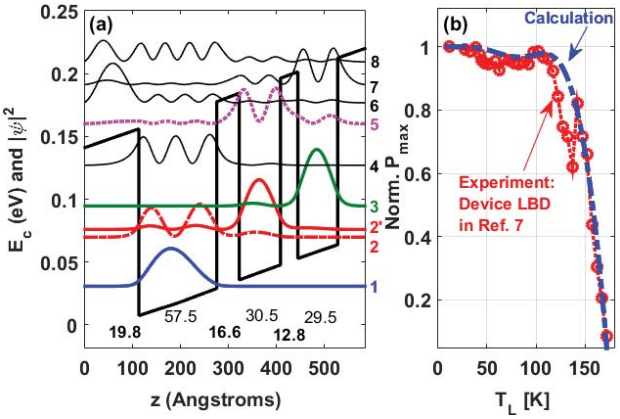

Fig. 2. (a) Conduction band profile of the device investigated in this work (LBD of Ref. [7]) under 13.4 kV/cm design electric field. Layer thicknesses in monolayers are indicated. Calculated design parameters are $E_3 - E_{2'} = h\nu = 16$ meV (photon energy), $f_{32'} = 0.17$ (oscillator strength) and $L_{mod} = 470$Å (module length). (b) Measured (red circles) and calculated (dashed-dotted blue line) normalized light output power as a function of temperature. The data is collected in pulsed operation mode and at low duty cycle in order to avoid self-heating. Further details to the device and to the experimental data can be found in the original publication [7].

scattering from the upper laser level (ULL) into the lower laser level (LLL) by thermally activated electron-LO-phonon interaction as unique temperature-sensitive process ([6], [7]).

We see from the calculation in Fig. 1 that thermally activated electron scattering from the ULL into the LLL by LO-phonons would lead to a nearly continuous decay of the output power as the temperature increases (dashed blue line); a trend characterized by an activation energy of $E_{LO} - h\nu \sim 20$ meV [6]. Any other thermally activated electron leakage mechanism –as understood in the traditional sense, i.e. one that reduces population inversion– added to the dashed blue line would result in lower output power values (see for example the dashed-doted green line in Fig 1). This expectation however clearly contradicts the experimental data for device LBD, which shows a nearly constant output power up to ∼120 K. In order to successfully explain the experimental results an additional temperature driven electron transport mechanism must exist, one that promotes population inversion as the temperature increases. To date, such a mechanism has not been identified.

In the present work we investigate the light output power vs. temperature profile of device LBD of [7] over the entire device operation temperature range 10 – 180 K. As mentioned above, the output power of this device is nearly constant up to a temperature of ∼120 K and it decreases rapidly for higher temperatures. We show that thermally activated leakage of carriers from the LLL into the continuum is the responsible mechanism for the observed stabilization of the output power up to ∼120 K.

II. Device Design and Modeling

Figure 2a shows the conduction band profile for a period of the investigated QCL design and Fig. 2b shows the measured normalized light output power as a function of temperature. The data is collected in pulsed mode with a low duty cycle in order to avoid self-heating effects. Further details on the device and measured data can be found in the original publication [7]. Fig. 2b includes also calculated values for the output power vs. temperature. These values are obtained modifying the method outlined in [6] and [9] in order include three temperature-sensitive electron scattering mechanisms, namely thermally activated LO-phonon scattering of electrons from the ULL into the LLL and thermally activated electron leakage from both the ULL and LLL into the continuum. The details of the calculations are developed in the following paragraphs.

Figure 3 shows the schematic representation of the energy levels and scattering paths of device LBD used for our analysis. We idealize in our approach the continuum as a virtual state wherefrom the carriers are assumed to be immediately recaptured in a non-lasing path back into the injector state of the next downstream cascade.[1] State 5 in Fig. 2a is assumed to be the excited state in device LBD that triggers escape into the continuum.

Based on earlier experimental studies (see for example [13]) we neglect thermal backfilling in our calculations. We further neglect the carrier leakage from the injector state (state 1 in Fig. 2a) into the continuum due its relatively high activation barrier. The doublet formed by the LLL and

[1]We base our approach on two arguments: (1) populations in QCL excited states are expected to be negligible with respect to active laser states' populations [10]–[12], which complements our assumption of immediate recapture into the next downstream cascade and (2) electron scattering from level 3 (or 2) into excited states is dominated by scattering into level 5 (the energetically and spatially closest state). This is equivalent to say that, at first order, the impact of electron leakage on the lifetime of state 3 (or 2) is represented by τ_{35} (τ_{25}). The effect of the virtual continuum state on the upper (and lower) laser state lifetime mimics the interaction between the continuum and active region bound states. Furthermore, the fact that this simple picture provides a reliable explanation of an observed physical effect (as the nearly constant light output power observed for device LBD up to 120 K) provides this assumption further support.

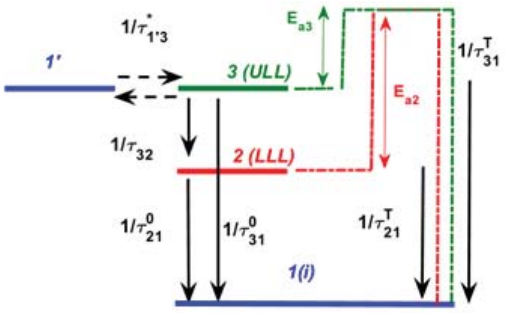

Fig. 3. Schematic representation of a 3-level QCL active region. Black arrows represent relevant non-radiative scattering paths with corresponding scattering times.[2] Energy levels are colored and labeled in analogy to Fig. 2a (levels 2' and 2 in Fig. 2a are treated as a single level 2 in Fig. 3). The dashed black arrows represent resonant tunneling transport between injector $1'$ and upper laser level 3 (ULL).[3] State $1(i)$ is the injector state of the next cascade. Vertical dashed-dotted lines represent energy barriers or activation energies $E_{a(2,3)}$ for escape into excited states that are strongly coupled with the continuum. After escaping into these states electrons are assumed to immediately relax into state $1(i)$.

the extractor levels, i.e., level 2' and 2 in Fig. 2a respectively, is treated as a single level 2 (LLL) in our calculations (Fig. 3). We would like to emphasize that our model is meant to provide a simple description of electron transport in THz-QCLs. Whereas more advanced models [14], [15] can be used for more elaborated description, we consider that our approach catches the essence of the underlying physics.

Electrons in the ULL and LLL (states $i = 3$ and $i = 2$ in Fig. 2a and Fig. 3) can reach the injector level of the next downstream cascade (state 1 in Fig. 2a and Fig. 3) in two ways: they can either scatter directly into state 1 by a characteristic time τ_{i1}^0 or scatter first into the continuum by a characteristic time τ_{i1}^T and then being captured into state 1. The total characteristic time for escape from the ULL and LLL is $\tau_{i1} = (\tau_{i1}^0 \tau_{i1}^T)/(\tau_{i1}^0 + \tau_{i1}^T)$, with i = ULL, LLL. τ_{i1}^0 is governed by electron-LO-phonon scattering[2]. The calculation of τ_{i1}^T is based on a thermionic emission model [17]–[19], resulting in the expression $\frac{1}{\tau_{i1}^T} = \frac{kT_{e_i}}{4h}\frac{N_{AV}^i}{N_i}$. Similarly to [17]–[19], we consider here the number of electrons $N_{AV}^i \approx (m^*/\pi\hbar^2)(kT_{e_i})T_{ic}\exp(-E_{a_i}/kT_{e_i})$ from level i that escaped into the continuum with respect to the total number of electrons N_i in that level.[4] E_{a_i} is the energy barrier (or activation energy), m^* is the electron effective mass in the quantum well material, k is the Boltzmann constant and $T_{e_i} = T_L + T_{ex_i}$ is the electron temperature of subband i, which is larger than the lattice temperature T_L ([20], [21]). T_{ex_i} is the electron excess temperature. T_{ic} is the total transmission coefficient associated with the specific excited resonance and barriers that are relevant for the escape process from level i into the continuum (calculated as in [15]).

The transmission coefficients for escape into the continuum through the excited state (level 5 in Fig. 2a) are calculated as $T_{3c} = \frac{T_{b1}T_{b2}}{T_{b1}+T_{b2}} = 0.063$ for electrons in the ULL and $T_{2c} = T_{b2} = 0.128$ for electrons in the LLL. T_{b1} (T_{b2}) is the transmission coefficient through barrier $b1$ ($b2$). $b1$ is the 12.8 monolayer-thick barrier and $b2$ is the 16.6 monolayer-thick barrier (Fig. 2a). As activation energies we use $E_{a_3} \approx 66$ meV and $E_{a_2} \approx E_{a_3} + h\nu \approx 82$ meV. These values correspond to the intersubband energy spacing between levels 3 and 5 for E_{a_3}, and 2' and 5 for E_{a_2} (Figure 2a).

The electron excess temperature T_{ex_i} is expected to decay with increasing lattice temperature [6], [9]. At low temperatures there is significant electron heating in all subbands due to the dominance of elastic scattering and, at higher temperatures, LO-phonon scattering becomes dominant and leads to an efficient cooling of electrons towards the lattice temperature. Calculations on several THz-QCL designs using resonant phonon extraction show that T_{ex_i} converges for $T_L > 100$K towards values as high as $T_{ex_3} \sim 0 - 20$ K for the ULL and $T_{ex_2} \sim 40 - 80$ K for the LLL. We use for simplicity T_{ex_3} and T_{ex_2} as temperature-independent yet subband-dependent fit parameters, which results in values as high as $T_{ex_3} = 0$ K and $T_{ex_2} = 45$ K for this particular device.

It is worth to mention that the effects of non-equilibrium LO-phonons are implicitly contained in our approach as we treat the subband electron temperatures as fitting parameters. Non-equilibrium LO-phonons generated during QCL operation would induce increased values of T_{ex_i} [22]. Furthermore, because of the low ($\sim 0.2 - 0.6$) occupation number of non-equilibrium LO-phonons in THz-QCLs ([23], [24]) we expect only a small impact of non-equilibrium LO-phonons on T_{ex_i} in our device.

Using these parameters, the output power is calculated using the method outlined in [6] and [9]. (The only additional calculation parameters are the gain bandwidth 1 THz and the total optical loss of 22 cm^{-1}, which are estimated from time domain spectroscopy data [25], [26]). Fig. 2b shows excellent agreement between calculation and experiment. We find that a variation of model parameters as the carrier density, injection tunneling time, gain bandwidth and total optical loss by $\pm$ 20% does not have a substantial impact on the calculation results and does not affect the conclusions of this work.

As next we discuss the impact of individual leakage paths on the output power.

III. Impact of Electron Leakage on Light Output Power

Figure 4 shows calculated light output power vs. temperature curves for device LBD under four different scenarios,

[2]Calculated non-radiative scattering times are $\tau_{31}^0 = 392$ ps and $\tau_{21}^0 = 0.81$ps. The former is the electron-LO-phonon scattering time from level 3 to level 1 (Fig. 2a and Fig. 3). The latter is the total scattering time from level 2' to level 1 (Fig. 2a). Note that electrons in level 2' can reach level 1 in two ways: they can either scatter directly into level 1 or scatter first into level 2 by resonant tunneling and then into level 1 by means of electron-LO-phonon scattering. The raw electron-LO-phonon scattering time [6] between levels 3 and 2' (Fig. 2a) is calculated to $\tau_{32}^0 = 1.69$ ps.

[3]The resonant-tunneling rates are calculated following [9] and [16] with a dephasing time $\tau_{pd} \approx 75$ *fs*, which is estimated analyzing the shape of low temperature current-voltage curves. Resulting values are $\tau_{1'3}^* = 5.4$ ps for resonant tunneling from the injector state (level 1' in Fig. 3) to the ULL (level 3 in Fig. 3) and $\tau_{2'2}^* = 0.88$ ps for resonant tunneling between levels 2' and 2 (Fig. 2a). $\tau_{2'2}^*$ is used in the calculation of τ_{21}^0.

[4]The populations of the upper and lower laser levels, N_3 and N_2, respectively, are estimated from rate equations calculations to $N_3 = 0.3\ N_{tot}$ and $N_2 = 0.06\ N_{tot}$, where $N_{tot} = 5.9 \times 10^{10}$cm^{-2} is the total sheet density per QCL period in device LBD [7].

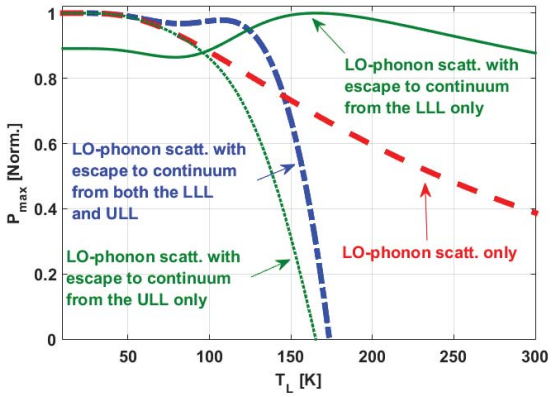

Fig. 4. Calculated light output power vs. temperature for device LBD in four different scenarios. The dashed red line represents complete suppression of carrier leakage from the ULL and LLL into the continuum. The dotted green line represents complete suppression of carrier leakage from the LLL into continuum. The solid green line represents complete suppression of carrier leakage from the ULL into continuum. The dashed blue line represents the combined effect of both thermally activated electron leakage from the ULL and LLL into the continuum and of thermally activated electron-LO-phonon scattering from the ULL into the LLL. The dashed blue line is the same curve as in Fig. 2b.

which are (1) complete suppression of carrier leakage from the ULL and LLL into the continuum (dashed red line), (2) complete suppression of carrier leakage from the LLL into continuum (dotted green line), (3) complete suppression of carrier leakage from the ULL into the continuum (solid green line) and (4) inclusion of carrier leakage from the ULL and LLL into the continuum and of thermally activated electron-LO-phonon scattering from the ULL into the LLL (dashed-dotted blue line). Scenario (4) is the same curve as in Fig. 2b.

Scenarios (1) and (2) exclude electron leakage from the LLL into the continuum and predict a continuously decaying output power as the temperature increases. This behavior remains however absent in the experimental data, which shows a nearly temperature-independent character up to $\sim$ 120 K (Fig. 2b). Fig. 4 shows that the apparent temperature-insensitivity of the device up to $\sim$ 120 K arises from the combined effects of electron leakage from the ULL and LLL into the continuum respectively and thermally activated electron-LO-phonon scattering from the ULL into the LLL. In this interplay, thermally activated leakage of carriers from the LLL into the continuum plays a key role as it is the only thermally activated scattering mechanism that leads (over a certain temperature range) to higher output powers as the temperature increases (solid green line). In other words, over a certain temperature range, thermally activated leakage of carriers from the LLL effectively compensates the reduced population inversion in the active region that arises from the other two leakage channels by means of a fast depopulation of the LLL. At higher temperatures, thermally activated leakage of carriers from the ULL into the continuum becomes dominant, deteriorating significantly the device performance.

An interesting consequence of this finding is that a full suppression of thermally activated leakage from the LLL into the continuum would lead to a reduced temperature performance of devices. This effect may explain the lower T_{max} values reported for THz-QCLs using high ($>$15% Al content) barriers with respect to low (15% Al content) barrier devices [8], [27]. This leakage mechanism may also explain the increase of the maximum output power that was observed in devices f26 and f30 of [28] as the temperature increased within the range 55 – 135 K ([28, Fig. 3a and 3b]).

IV. Conclusion

In conclusion, thermally activated leakage of electrons from the lower laser level into the continuum can be fast enough to effectively counteract the population inversion decrease that arises from the remaining electron leakage channels as the temperature increases. This effect leads to a higher output power by means of an enhancement of the stimulated emission rate with temperature increase and contributes significantly to the performance of state of the art devices. This finding opens the question if new design approaches for THz-QCLs that exploit this effect can be developed in order to demonstrate devices with higher T_{max}. This work is the first demonstration of a thermophotonic mechanism in semiconductor lasers, which utilizes generated heat in order to increase the number of coherent photons. A similar effect has been recently reported for infrared- and blue-light emitting diodes [29],[30].

Acknowledgment

The authors would like to thank Prof. Qing Hu for the devoted mentoring, the many enlightening discussions and for his generous support in performing this research. A. A. would like to acknowledge the generosity and support of the MIT-Technion and the Andrew and Erna Finci Viterbi Fellowships. Y. V. F. acknowledges the support of the Research Fellowship Program of the German Research Foundation, DFG (Grant FL945/1-1).

References

[1] U. S. Fathololoumi *et al.*, "Terahertz quantum cascade lasers operating up to ~200 K with optimized oscillator strength and improved injection tunneling," *Opt. Exp.*, vol. 20, no. 4, pp. 3866–3876, 2012.

[2] D. Botez, C.-C. Chang, and L. J. Mawst, "Temperature sensitivity of the electro-optical characteristics for mid-infrared (λ = 3-16 m)-emitting quantum cascade lasers," *J. Phys. D, Appl. Phys.*, vol. 49, no. 4, p. 43001, 2016.

[3] Y. V. Flores *et al.*, "Thermally activated leakage current in high-performance short-wavelength quantum cascade lasers," *J. Appl. Phys.*, vol. 113, no. 13, p. 134506, 2013.

[4] Y. V. Flores, S. S. Kurlov, M. Elagin, M. P. Semtsiv, and W. T. Masselink, "Leakage current in quantum-cascade lasers through interface roughness scattering," *Appl. Phys. Lett.*, vol. 103, no. 16, p. 161102, 2013.

[5] C. Pflügl *et al.*, "Activation energy study of electron transport in high performance short wavelengths quantum cascade lasers," *Opt. Exp.*, vol. 18, no. 2, pp. 746–753, 2010.

[6] A. Albo and Q. Hu, "Investigating temperature degradation in THz quantum cascade lasers by examination of temperature dependence of output power," *Appl. Phys. Lett.*, vol. 106, no. 13, p. 131108, 2015.

[7] A. Albo and Q. Hu, "Carrier leakage into the continuum in diagonal GaAs/$Al_{0.15}$GaAs terahertz quantum cascade lasers," *Appl. Phys. Lett.*, vol. 107, no. 24, p. 241101, 2015.

[8] A. Albo, Q. Hu, and J. L. Reno, "Room temperature negative differential resistance in terahertz quantum cascade laser structures," *Appl. Phys. Lett.*, vol. 109, no. 8, p. 081102, 2016.

[9] C. W. I. Chan, "Towards room-temperature terahertz quantum cascade lasers: Directions and design," Ph.D. dissertation, Dept. Elect. Eng. Comput. Sci., Massachusetts Inst. Technol., Cambridge, MA, USA, 2015.
[10] K. A. Krivas, D. O. Winge, M. Franckié, and A. Wacker, "Influence of interface roughness in quantum cascade lasers," *J. Appl. Phys.*, vol. 118, no. 11, p. 114501, 2015.
[11] Y. V. Flores, S. S. Kurlov, M. Elagin, M. P. Semtsiv, and W. T. Masselink, "The role of electron temperature in the leakage current in QCLs and its impact on the quantum efficiency," *Proc. SPIE*, vol. 9002, p. 90021R, Feb. 2014.
[12] S. S. Kurlov *et al.*, "Phenomenological scattering-rate model for the simulation of the current density and emission power in mid-infrared quantum cascade lasers," *J. Appl. Phys.*, vol. 119, no. 13, p. 134501, 2016.
[13] B. S. Williams, S. Kumar, Q. Qin, Q. Hu, and J. L. Reno, "Terahertz quantum cascade lasers with double-resonant-phonon depopulation," *Appl. Phys. Lett.*, vol. 88, no. 26, p. 261101, 2006.
[14] P. Harrison and A. Valavanis, *Quantum Wells, Wires and Dots: Theoretical and Computational Physics of Semiconductor Nanostructures*, 4th ed. West Sussex, U.K.: Wiley, 2016.
[15] J. Faist, *Quantum Cascade Lasers*. Oxford, U.K.: Oxford Univ. Press, 2013.
[16] R. F. Kazarinov and R. A. Suris, "Possibility of amplification of electromagnetic waves in a semiconductor with a superlattice," *Soviet Phys. Semicond.*, vol. 5, no. 4, pp. 707–709, 1971.
[17] H. Schneider and K. V. Klitzing, "Thermionic emission and Gaussian transport of holes in a GaAs/Al_xGa_{1-x}As multiple-quantum-well structure," *Phys. Rev. B*, vol. 38, no. 9, pp. 6160–6165, Sep. 1988.
[18] M. Irikawa, T. Ishikawa, T. Fukushima, H. Shimizu, A. Kasukawa, and J. Iga, "Improved theory for carrier leakage and diffusion in multiquantum-well semiconductor lasers," *Jpn. J. Appl. Phys.*, vol. 39, no. 4A, p. 1730, 2000.
[19] A. Albo, G. Bahir, and D. Fekete, "Improved hole confinement in GaInAsN–GaAsSbN thin double-layer quantum-well structure for telecom-wavelength lasers," *J. Appl. Phys.*, vol. 108, no. 9, p. 093116, 2010.
[20] P. Harrison, D. Indjin, and R. W. Kelsall, "Electron temperature and mechanisms of hot carrier generation in quantum cascade lasers," *J. Appl. Phys.*, vol. 92, no. 11, pp. 6921–6923, 2002.
[21] M. S. Vitiello *et al.*, "Measurement of subband electronic temperatures and population inversion in THz quantum-cascade lasers," *Appl. Phys. Lett.*, vol. 86, no. 11, p. 111115, 2005.
[22] Y. B. Shi and I. Knezevic, "Nonequilibrium phonon effects in mid-infrared quantum cascade lasers," *J. Appl. Phys.*, vol. 116, no. 12, p. 123105, 2014.
[23] J. T. Lü and J. C. Cao, "Monte Carlo simulation of hot phonon effects in resonant-phonon-assisted terahertz quantum-cascade lasers," *Appl. Phys. Lett.*, vol. 88, no. 6, p. 061119, 2006.
[24] M. S. Vitiello *et al.*, "Non-equilibrium longitudinal and transverse optical phonons in terahertz quantum cascade lasers," *Appl. Phys. Lett.*, vol. 100, no. 9, p. 091101, 2012.
[25] D. Burghoff, T.-Y. Kao, D. Ban, A. W. M. Lee, Q. Hu, and J. Reno, "A terahertz pulse emitter monolithically integrated with a quantum cascade laser," *Appl. Phys. Lett.*, vol. 98, no. 6, p. 061112, 2011.
[26] D. Burghoff, C. W. I. Chan, Q. Hu, and J. L. Reno, "Gain measurements of scattering-assisted terahertz quantum cascade lasers," *Appl. Phys. Lett.*, vol. 100, no. 26, p. 261111, 2012.
[27] T.-T. Lin, L. Ying, and H. Hirayama, "Threshold current density reduction by utilizing high-al-composition barriers in 3.7 THz GaAs/Al_xGa_{1-x}As quantum cascade lasers," *Appl. Phys. Exp.*, vol. 5, no. 1, p. 012101, 2012.
[28] S. Fathololoumi *et al.*, "Effect of oscillator strength and intermediate resonance on the performance of resonant phonon-based terahertz quantum cascade lasers," *J. Appl. Phys.*, vol. 113, no. 11, p. 113109, 2013.
[29] P. Santhanam, D. J. Gray Jr., and R. J. Ram, "Thermoelectrically pumped light-emitting diodes operating above unity efficiency," *Phys. Rev. Lett.*, vol. 103, p. 097403, 2012.
[30] J. Xue, Y. Zhao, S.-H. Oh, W. F. Herrington, and J. S. Speck, "Thermally enhanced blue light-emitting diode," *Appl. Phys. Lett.*, vol. 107, p. 121109, 2015.

Asaf Albo received the B.Sc. degrees (Hons.) in physics and materials engineering from the Technion, Israel Institute of the Technology in 2002, the M.Sc. degree from the Department of Materials Engineering, Technion, Israel Institute of the Technology, in 2005, and the Ph.D. degree from the Department of Electrical Engineering, Technion, Israel Institute of the Technology, in 2011, He was a Research and Development Senior Physicist in the semiconductor industry for about four years. He is currently a Research Associate with the Research Laboratory of Electronics, Massachusetts Institute of Technology, where he studies the temperature performance of terahertz quantum cascade lasers and develops novel design concepts to improve their maximum operating temperature. He is also a Materials and Devices Researcher that specializes in semiconductors, quantum-structures and their optoelectronic devices.

Yuri V. Flores was born in Baku, Azerbaijan, in 1986. He received the B.Sc. degree from the Leibniz University of Hannover, Hannover, Germany, in 2010, and the M.Sc. degree and the Ph.D. degree (Highest Hons.) from Humboldt University Berlin, Germany, in 2013 and 2015, respectively, all in physics. He gained work experience at the Institute of Transport- and Automation Technology, Hannover, and the Ferdinand-Braun-Institute, Leibniz Institute for High-Frequency Technology, Berlin. His research at Humboldt University focused on the development of a realistic model for the description of electron transport in mid-infrared quantum cascade lasers (QCLs), which led to the development of novel experimental and theoretical approaches to investigate thermally-activated electron leakage phenomena. He has authored or co-authored 20 technical papers. He is currently a Post-Doctoral Research Fellow with the Research Laboratory of Electronics, Massachusetts Institute of Technology, where he is involved in the development of novel design concepts for terahertz-emitting QCLs.